References and Notes

1. R. Etkins and E. S. Epstein, *Science* **215**, 287 (1982); R. R. Revelle, in *Changing Climate* (National Academy of Sciences, Washington, D.C., 1983), pp. 443–448; A. Robock, *Science* **219**, 996 (1983).
2. V. Gornitz, S. Lebedeff, J. Hansen, *Science* **215**, 1611 (1982).
3. T. P. Barnett, *Clim. Change* **5**, 15 (1983).
4. M. F. Meier, *Hydrol. Sci. J.* **28**, 3 (1983).
5. C. R. Bentley, in *Climate Processes and Climate Sensitivity*, J. E. Hansen and T. Takahashi, Eds. (Maurice Ewing Series 5, American Geophysical Union, Washington, D.C., 1984), pp. 207–220.
6. U. Radok *et al.*, *Climatic and Physical Characteristics of the Greenland Ice Sheet* (Cooperative Institute for Research in Environmental Sciences, Boulder, Colo., 1982); R. A. Bindschadler, *J. Geophys. Res.* **89**, 2066 (1984).
7. International Association of Scientific Hydrology, *Tech. Pap. Hydrol.* **5** (1970); L. R. Mayo *et al.*, *J. Glaciol.* **11**, 3 (1972). The distinction between annual and net balances, important for a given year, becomes unimportant for the long time series discussed here.
8. In some cases G_0 is not given; in others only mean thickness change is given. In these cases only G_1 is known and the resulting $\bar{b}$ is underestimated.
9. W. V. Tangborn, *J. Glaciol.* **25**, 3 (1980).
10. At least one uncalibrated HM model gives a long-term $\bar{b} > 0$ for a glacier that was shrinking.
11. However, the changing glacier area $G(t)$ must be known to translate $b(t)$ to meltwater volume; this is generally not reported, resulting in an underestimate similar to that described in (*8*).
12. International Association of Scientific Hydrology, *Fluctuations of Glaciers* (Unesco, Paris, 1967), vol. 1; *ibid.* (1973), vol. 2; *ibid.* (1977), vol. 3.
13. M. F. Meier, unpublished compendium of data sources.
14. Quality weights used are 4/7 for calibrated HM models and high-quality volume change observations, 2/7 for other volume change observations, and 1/7 for volume change estimates and uncalibrated HM models.
15. In areas of monsoon climate and in some high polar areas, the expression $a = (|b_w| + |b_s|)/2$ was used.
16. R. Koerner (unpublished manuscript) notes that many ice caps and outlet glaciers in arctic Canada show no measurable change in the last several decades; others show thinning, areal shrinkage, or retreat, especially during the period 1950 to 1970. Some small ice caps have disappeared, but the changes are "not especially dramatic."
17. The a_j and a_k in Eq. 4 represent average values during the period 1965 to 1975 (in some cases, even shorter periods), which was a period of extensive measurement. These values are used as estimates of unknown longer term average values $\bar{a}$. Because it seems unlikely that the a_j would have varied as much through time as b_j, the error introduced is probably small.
18. The estimated standard error is the combination of variances in all data sets used in Eq. 4 (±0.25 mm/year), plus an estimate of the error due to sometimes unknown decreases in area (±5 percent).
19. S. Thorarinsson [*Geogr. Ann.* **22**, 131 (1940)] estimated a similar rate of sea level rise due to glacial shrinkage in the 1920's and 1930's.
20. L. Renaud, *Int. Assoc. Sci. Hydrol. Publ. 126* (1980), p. 273.
21. For the period 1965–75, correlation coefficients for the average annual balances between pairs of ten regions range from −0.44 to +0.53. For seven long-term balance series, all in different regions, the correlation coefficients range from −0.48 to +0.45. O. Orheim [*Ohio State Univ. Inst. Polar Stud. Rep. 42* (1972)] notes that using 10-year moving averages greatly improves the correlations.
22. O. Liestøl, *Storbreen Glacier in Jotunheim, Norway* (Norsk Polarinstitutt, Oslo, 1967), p. 141.
23. S. Martin, *Zeit. Gletscherkunde u. Glazialgeologie* **13**, 127 (1978).
24. J. Hansen *et al.*, *Science* **213**, 957 (1981); G. Weller *et al.*, in *Changing Climate* (National Academy of Sciences, Washington, D.C., 1983), pp. 292–382.
25. L. Machta, in *Changing Climate* (National Academy of Sciences, Washington, D.C., 1983), pp. 262–265.
26. Climate Research Board, *Carbon Dioxide and Climate—A Scientific Assessment* (National Academy of Sciences, Washington, D.C., 1979); *Carbon Dioxide and Climate—A Second Assessment* (National Academy of Sciences, Washington, D.C., 1982).

27. I thank S. Ommaney, R. Koerner, V. Kotliakov, and P. Holmlund for access to unpublished material, Cao Meisheng for help in translation of Chinese sources, B. Vaughn and D. Smith for assisting in data compilation, L. A. Rasmussen for much helpful discussion, J. Hansen, L. A. Rasmussen, and C. R. Bentley for useful manuscript reviews, an anonymous reviewer for locating a numerical error, and T. P. Barnett who suggested that I look into this question.

19 April 1984; accepted 25 July 1984

A Circumstellar Disk Around β Pictoris

Abstract. *A circumstellar disk has been observed optically around the fourth-magnitude star β Pictoris. First detected in the infrared by the Infrared Astronomy Satellite last year, the disk is seen to extend to more than 400 astronomical units from the star, or more than twice the distance measured in the infrared by the Infrared Astronomy Satellite. The β Pictoris disk is presented to Earth almost edge-on and is composed of solid particles in nearly coplanar orbits. The observed change in surface brightness with distance from the star implies that the mass density of the disk falls off with approximately the third power of the radius. Because the circumstellar material is in the form of a highly flattened disk rather than a spherical shell, it is presumed to be associated with planet formation. It seems likely that the system is relatively young and that planet formation either is occurring now around β Pictoris or has recently been completed.*

To the unaided eye, β Pictoris is a rather inconspicuous star in an equally obscure constellation and, located at far southerly declinations, it remains permanently below the horizon to much of Earth's Northern Hemisphere. At a distance of 16 parsecs (53 light-years), this fourth-magnitude star is considered a member, albeit somewhat remote, of the immediate solar neighborhood; it is classified as a main-sequence dwarf, similar to the sun in an evolutionary sense, but with twice the mass and probably ten times the luminosity (*1*). Interest in β Pictoris has increased greatly during the past year; observations by the Infrared Astronomy Satellite (IRAS) have led the IRAS investigator team to the conclusion that this star is surrounded by a cloud of cold, solid material, possibly in the form of a circumstellar disk (*2*). The IRAS investigators have also concluded that circumstellar material may be present around as many as one star in every five or ten and have suggested that, in the case of one of the stars (α Lyrae), the material may be associated with planet formation. Recently, we were successful in obtaining optical images of the disk, confirming its existence and tracing its extent from β Pictoris to more than twice the distance observed by IRAS.

Our observations were made at the Las Campanas Observatory (*3*) in Chile on 15 to 18 April 1984, using the du Pont 2.5-m telescope, a CCD camera (*4*), and a special optical instrument known as a coronagraph (*5*). The images of β Pictoris and those of a similar comparison star, α Pictoris, were taken through an optical filter centered at a wavelength of 890 nm, in the far-red region of the spectrum. The specially designed coronagraph was used to eliminate the starlight scattered into the immediate vicinity of the stellar image by diffraction from within the telescope, particularly that component of diffracted light created by the support structure for the telescope's secondary mirror. The coronagraph also contained a small (7 arcsec) circular mask positioned in the focal plane of the telescope to block out most of the light from the star. All data were digitized to an intensity range of 16 bits per pixel and recorded on magnetic tape.

The images obtained in Chile have been processed on both a Vicom image processing system at the University of Arizona and a similar DeAnza system at the Image Processing Laboratory of the Jet Propulsion Laboratory. After correcting for instrumental response and subtracting the contribution from the sky background, a series of ratio and difference images were created from normalized β and α Pictoris image pairs. Use of the α Pictoris images to correct for the scattered light around β Pictoris is made necessary by the relatively large difference between the brightness of the atmospherically scattered light from the star and the surface brightness of the disk itself. Even with the coronagraph, the scattered light from β Pictoris is three to five times brighter than the disk over most of the observable range. Were this not the case, the disk would surely have been discovered long ago by using conventional techniques with optical telescopes.

One example of the ratio images is shown in Fig. 1. The β Pictoris disk can be seen extending radially outward from the star, which was positioned behind the focal plane mask. The small spots appearing in Fig. 1 are positive (light) and negative (dark) images of faint field

stars recorded along with β and α Pictoris, respectively. The dark vertical and horizontal lines centered on the mask are 10-μm silk monofilaments, which were used to support the mask in the focal plane. Other light and dark vertical stripes are caused by minor defects in the CCD chip. From the appearance in Fig. 1, one can tell immediately that the disk is being presented nearly edge-on as seen from Earth, that is, that the plane of the disk is within a few degrees of being perpendicular to the plane of the sky (*6*). Such a fortuitous orientation contributes significantly to the conspicuousness, and perhaps even the optical detectability, of the β Pictoris disk.

Because of edge effects around the obscuring focal plane mask, we cannot make reliable photometric measurements of the disk any closer to β Pictoris than about 100 AU (*7*). At this distance, the far-red disk brightness is approximately 16th magnitude per square arcsec, falling off monotonically with increasing distance from the star (Fig. 2). More specifically, the edge-on disk surface brightness decreases with the 4.3 power of its distance from β Pictoris; this power-law relationship holds remarkably well over the range from 100 to 400 AU.

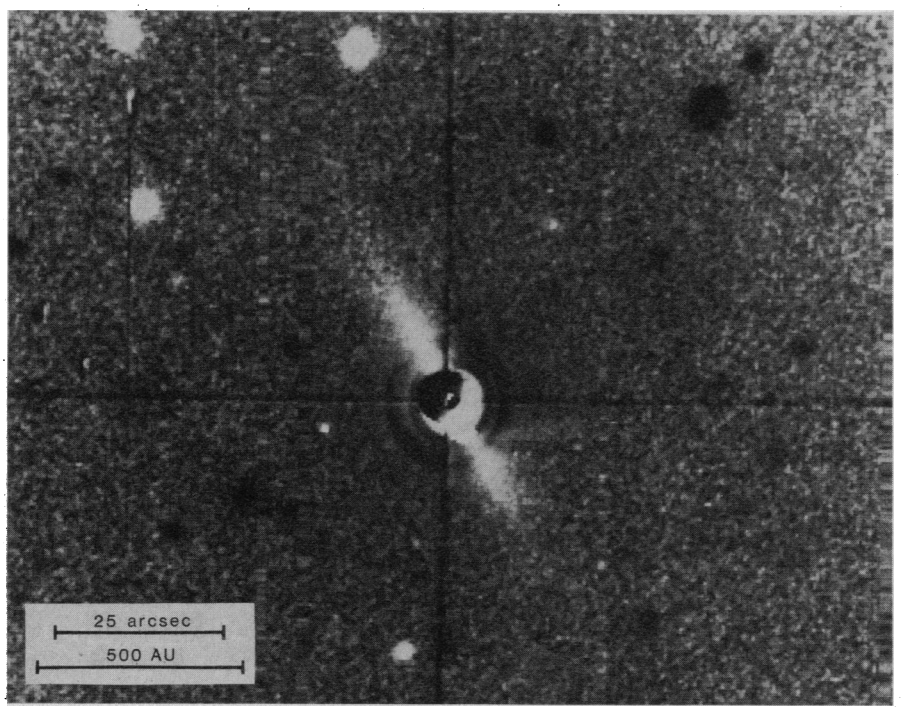

Fig. 1. Ratio image (β Pictoris divided by α Pictoris) showing the edge-on circumstellar disk extending 25 arcsec (400 AU) to the northeast and southwest of the star, which is situated behind an obscuring mask. North is at the top. The dark halo surrounding the mask is caused by imperfect balance in the ratioing process. For further explanation, see text.

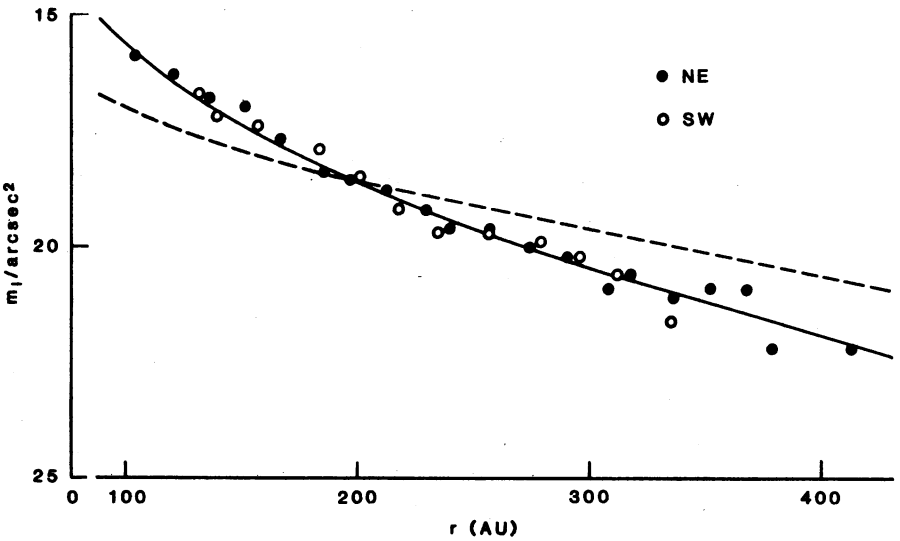

Fig. 2. Integrated surface brightness of the β Pictoris disk seen in projection against the plane of the sky. The solid and open circles are measured points along the northeast and southwest extensions, respectively. Surface brightness is in I (890-nm) magnitudes per square arcsec and the radius from the star is given in astronomical units. The dashed and solid lines are computer surface brightness from models in which the number density of disk particles falls off inversely and with the negative third power of the radial distance, respectively.

With no knowledge at this time of the size distribution or scattering properties of the disk particles, or how these parameters may change with location throughout the disk, we cannot rigorously derive either the optical thickness or mass distribution within the β Pictoris disk. The application of certain simplifying constraints on both the physical properties and size distribution of the scattering particles, however, allows construction of a model fitting the observed disk brightness as a function of distance and, thereby, the approximate optical thicknesses and distribution of mass within the disk. We now proceed with the assumption that the disk material, which is made visible by scattered starlight, can be represented by a swarm of high-albedo, diffusely reflecting, unit density, spherical particles with a particle size distribution that is invariant throughout the observable disk. In the model, the mean particle size is not important, provided it is significantly greater than the wavelength of light, that is, several micrometers. We will demonstrate later that this condition is met. At each point along the axis of the projection of the disk on the plane of the sky, the observed brightness is a summation of contributions from many points within the disk, each with its individual number of scattering particles per unit volume, $n(r)$, at distance r from the star, and each subject to the inverse square law of illumination from the star. To further facilitate these preliminary calculations, we assume that $n(r)$ can also be represented by a power-law function of its distance from the star, that nonlinear terms in the single-particle scattering phase function can be ignored, and that only single scattering is involved. This last condition requires that the disk be optically thin, even when viewed in its nearly edge-on presentation.

The solid and dashed lines in Fig. 2 are calculated brightnesses from two models; the solid line represents a disk model in which the number density $n(r)$ decreases as $r^{-3.1}$ and, for comparison, the

dashed line shows a case in which $n(r)$ decreases linearly with distance from the star. The solution in which $n(r)$ decreases with approximately the third power of the distance is based on a disk radius of 500 AU and is seen to fit the observations quite well. Although uniqueness can hardly be claimed for any particular model, we conclude that the distribution of mass per unit volume within the disk must be proportional to approximately r^{-3}. The model also predicts both the local dimensionless scattering cross section $\sigma(r)$ per unit length as a function of position within the disk and the integrated optical thickness $\tau(r)$ for a chord across the disk, as shown in Fig. 3. Here, σ is defined by $d\tau(x) = \sigma(x)dx$. The lower curve in Fig. 3 is the scattering cross section $\sigma(r)$ per astronomical unit within the disk at distance r in astronomical units from β Pictoris. The upper curve is the integrated optical thickness $\tau(r)$ along a chord that passes closest to the star at the indicated distance. The values in this upper curve support our computational constraint that the disk be optically thin ($\tau < 0.1$) over the observable range.

Without additional observations, we cannot say what happens within 100 AU, but we do note that if the disk material were to continue inward toward β Pictoris and if the adopted scattering properties and radial distribution $n(r)$ were to remain applicable, the integrated chord through the disk would become optically thick ($\tau \sim 1$) at about 15 AU. As the geometry in the images indicates, we are viewing β Pictoris through its own disk and, therefore, can make some estimate of the total radial optical thickness of the disk. At the assumed distance of the star (*1*, *7*), its brightness is about 0.5 magnitude fainter than the average star in its spectral or color classification (*8*). If this difference is statistically significant, it would suggest a total radial optical thickness of about 0.5 and, if the model could still be applied to the inner part of the β Pictoris system, it would imply that the disk extends inward only to about 30 AU and that the region within 30 AU is relatively clear. It is also important to note that multicolor photometry of β Pictoris shows no significant reddening (*1*) and that this is indicative of neutral extinction, that is, extinction by particles large compared to the wavelength of light. This supports one of the model assumptions stated earlier.

As can be seen in Figs. 1 and 2, the circumstellar disk around β Pictoris extends to at least 400 AU and, according to the model, possibly to 500 AU; this is more than ten times the mean distance from the sun of the most remote known planet within our own solar system (*9*). The disk also becomes geometrically thicker with increasing distance from the star. When allowances are made for the finite resolution of the image (*10*), we find a geometrical thickness of about 50 AU at a distance of 300 AU; this implies that the orbits of most of the disk particles are inclined 5° or less to the plane of the system. Such small orbital inclinations to the invariable plane are typical of the major planetary bodies within our own solar system, and because the orbits of these larger bodies are not easily perturbed, they tend to retain the memory of those inclinations which existed early within the solar protoplanetary disk. As the solar system has evolved, smaller bodies such as comets and asteroids have been perturbed into orbits of higher inclination. The perturbing masses within the inner part of the solar system have been the planets, primarily Jupiter and Saturn, while farther out the most likely candidates have been passing stars and giant molecular clouds (*11*). However, the probability of one star passing sufficiently close to another to disturb particles at distances of only a few hundred astronomical units is vanishingly small over the lifetime of β Pictoris system (*11*). Therefore, without a detailed knowledge of the existence of large bodies or their distribution within the β Pictoris system, we cannot estimate the time scale for stirring up the orbital elements of the observed disk particles. Nevertheless, the retention of nearly coplanar orbits in the β Pictoris disk is a qualitative argument in support of its being a relatively young system.

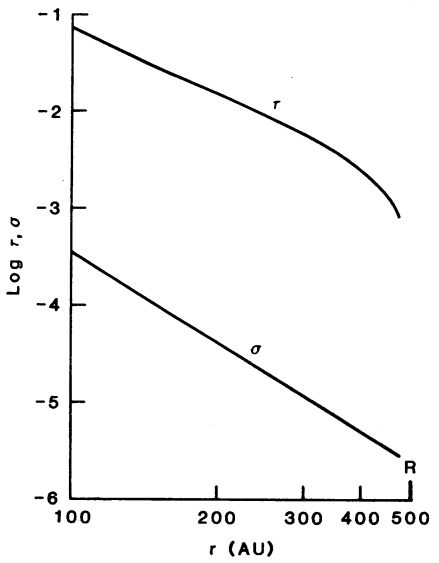

Fig. 3. Model-dependent values for the local dimensionless scattering cross section per astronomical unit in the β Pictoris disk (bottom curve) and the integrated optical thickness along a chord that passes through the disk (top curve), as a function of radius r. For the top curve, r is the distance at which the chord passes closest to the star; R is the edge of the disk in the model.

The composition of the β Pictoris disk is not known from the data presently available, but part or nearly all of its mass might be in the form of small grains composed of silicates, carbonaceous material, and ices, primarily water ice. Molecular hydrogen might also be expected, but only the solid disk material is visible in our images, and the same would be true of the IRAS observations (*2*). In addition, we consider the possibility that part of the visible mass is in the form of relatively large particles in the kilometer range, as would be expected if the β Pictoris system contained some radial distribution of comet nuclei. For this size distribution, we again use a power law, $dn(a) \propto a^{-3.5}da$ (*12*), where $dn(a)$ is the relative number of particles having a diameter between a and $a + da$; the upper and lower limits of the particle size distribution are somewhat arbitrarily taken to be 10 km and 10 μm, respectively. Without additional observational data, we cannot distinguish among various characteristic particle sizes (micrometers to kilometers), or other distributions such as a power law. It is possible, however, to estimate the total mass and angular momentum in the disk beyond 100 AU both for grain size particles, say 10 μm, and for the power-law distribution given above. For these two examples, the estimates of the mass of the disk from 100 to 500 AU are 4×10^{25} and 10^{30} g, respectively; the corresponding values for angular momentum are 4×10^{46} and 10^{51} g cm^{-2} sec^{-1}. Thus, for the two models, the estimates of the total mass in the disk from 100 AU outward are 0.01 and 200 Earth masses and of the total angular momentum are 2×10^{-8} and 5×10^{-4} times the rotational angular momentum of β Pictoris itself (*13*).

The observational evidence that circumstellar material around β Pictoris takes the form of a highly flattened disk rather than a spherical shell implies an almost certain association with planet formation. Although there is no direct evidence to support the existence of a planetary system around β Pictoris, the disk material itself represents a potential source for planet accretion. The disk material visible in the observations, of course, extends well beyond the regions within a few tens of astronomical units of

the star where planets might be expected to form. The disk might consist of outlying debris remaining after an inner accretionary phase, but it might also include inner material ejected outward by planets already formed. It is estimated that the time required for planet formation is relatively brief; 10^8 years is a characteristic time scale (*14*). This, however, is much longer than 3×10^6 years, the time required for a two-solar-mass star to reach the main sequence following its collapse from a cloud of gas and dust (*15*). Thus, as a main-sequence star of indeterminate age, β Pictoris may or may not have been in existence long enough to have formed a system of planets. However, we have already concluded that the disk mass does not extend inward to regions of high optical thickness, and this would imply a mechanism for depleting material within a few tens of astronomical units around the star. Two likely mechanisms are the Poynting-Robertson effect (*16*) and accretion of the depleted material into planetary bodies. Using our assumed mass and luminosity for β Pictoris (*1*), we find that particles smaller than 100 μm could be removed from the region within 30 AU of the star over an interval of 10^7 years and that 0.1-cm particles could be depleted in 10^8 years. Furthermore, over an interval of slightly more than 10^8 years, 10-μm particles could be totally depleted from all regions out to the visible limits of the disk. However, small particles can also be replenished by mechanisms such as collisions between larger particles or by the ejection of cometary material, as has been suggested to explain the α Lyrae (Vega) circumstellar material (*17*). Since we do not know the details of the source mechanisms, we cannot predict the evolution of the distribution of small particles (0.001 to 0.1 cm) from the region within a few tens of astronomical units from β Pictoris. Larger particles, however, could be removed only through the planetary accretion process; this is just what happened within a volume of similar size in our own solar system.

We do not know the age of β Pictoris, only that it must be younger than its main-sequence lifetime of approximately 10^9 years (*15*). As stated earlier, however, the nearly coplanar, low-inclination orbits of the disk particles are an indication of a stellar system that has not yet evolved much beyond zero age on the main sequence. It is tempting to speculate, therefore, that we may be witnessing ongoing planetary formation around β Pictoris or, alternatively, that we are viewing the distant detritus of an already extant but young system of planets. Further observations of β Pictoris and studies of other circumstellar disks may be helpful in determining what role, if any, is played by remote circumstellar material in the formation of planetary systems.

Both infrared and optical instruments are useful in searching for circumstellar material. Infrared instruments generally have far less angular resolution than optical ones but, because they observe reradiated energy in the thermal infrared, emission from circumstellar material tends to stand out against the relatively weak, long-wavelength radiation from the star itself. At great distances from the star, however, circumstellar material becomes too cold to be detected by infrared techniques. Optical instruments, on the other hand, see only scattered starlight, and thus tend to work best in the same spectral region in which the star radiates most of its energy. This, of course, limits the ability of optical instruments to see material close to the star itself, but their ability to detect circumstellar material at large distances is limited only by angular resolution and by the contrast of the material's surface brightness against the sky background. In the case of β Pictoris, as we have already noted, the optical detection extends to twice the distance of the infrared.

The IRAS investigators have found excess thermal radiation from a surprisingly large number of nearby stars, suggesting that circumstellar material may be commonplace in the galaxy. Telescopes with optical coronagraphs, operating both from Earth's surface and later from space, should be able to image many of these circumstellar shells or disks and thereby determine their morphology and spatial distribution of material. Such studies may shed new light on the formation and evolution of planetary systems.

BRADFORD A. SMITH
Department of Planetary Sciences, University of Arizona, Tucson 85721
RICHARD J. TERRILE
Jet Propulsion Laboratory, Pasadena, California 91109

References and Notes

1. Beta Pictoris has a visual magnitude of 3.85, a spectral classification of A5V (main sequence), a rotational velocity of 139 km sec^{-1}, and a parallax of 0.061 arcsec, according to the *Bright Star Catalog*, D. Hoffleit, Ed. (Yale University Observatory, New Haven, Conn., 1982). Additional photometric information can also be found in this publication.
2. Beta Pictoris is one of four stars announced by the IRAS investigator team to be surrounded by circumstellar material; the others are α Lyrae (Vega), α Piscis Austrini (Fomalhaut), and ε Eridani. See, for example, H. H. Aumann, F. C. Gillett, C. A. Beichman, T. de Jong, J. R. Houck, F. Low, G. Neugebauer, R. G. Walker, P. Wesselius, *Astrophys. J. Lett.* **278**, L23 (1984); B. M. Schwarzschild, *Phys. Today* **37** (No. 5), 17 (1984); H. H. Aumann, *Bull. Am. Astron. Soc.* **16**, 483 (1984).
3. The Las Campanas Observatory is operated by the Carnegie Institution of Washington. We were guest observers in April 1984.
4. The CCD (charge-coupled device) camera used in these observations was a development instrument made available by the Hubble Space Telescope Wide Field/Planetary Camera Instrument Definition Team. One of us (B.A.S.) is a member of the WF/PC team.
5. The coronagraph that we used is a modification of the basic instrument designed by B. Lyot more than 50 years ago [B. Lyot, *Mon. Not. Astron. Soc.* **99**, 580 (1939); see also F. Vilas, thesis, University of Arizona (1984)]. This instrument has proved to be especially capable in detecting faint objects in the immediate vicinity of very bright sources.
6. Bipolar outflow, a phenomenon associated with young, pre–main-sequence stars, can be eliminated as an explanation of the image because β Pictoris is an established main-sequence star. Furthermore, reflections within the coronagraph cannot explain the observations; images of other stars recorded during the same observing run are symmetrical.
7. The astronomical unit (AU) is the mean distance of Earth from the sun, 149.6 million kilometers. Although the actual distance of β Pictoris has an associated uncertainty of about 15 pecent, we use the value of 16.4 parsecs, equivalent to the parallax cited in (*1*). At a distance of 16.4 parsecs, 1 arcsec equals 16.4 AU.
8. The apparent brightness of β Pictoris viewed through its disk is about 0.8 magnitude fainter than a typical A5V star and 0.3 magnitude fainter than a similar zero-age main-sequence star [see C. W. Allen, *Astrophysical Quantities* (Athlone, London, 1973). The distance uncertainty given in (*7*) corresponds to an intrinsic brightness uncertainty of 0.3 magnitude. Neither the age of β Pictoris nor its precise distance is known; we, therefore, adopt a brightness difference of 0.5 magnitude.
9. At present, Neptune, at 30 AU, is the most distant planet from the sun. In approximately 125 years, Pluto, whose mean orbital radius is 39 AU, will reach its maximum distance of nearly 50 AU.
10. The width at half-maximum of the point-spread function (instrumentally and atmospherically induced blurring of a point source) averages about 1.2 arcsec in our images. This is equivalent to 20 AU at the distance of β Pictoris.
11. J. H. Oort, *Bull. Astron. Inst. Neth.* **11**, 91 (1950); A. G. W. Cameron, *The Origin of the Solar System*, S. F. Dermott, Ed. (Wiley, New York, 1978); M. E. Bailey, *Mon. Not. R. Astron. Soc.* **204**, 603 (1984); see also J. G. Hills, *Astron. J.* **89**, 1559 (1984).
12. Here we have used the power-law size distribution for asteroids given by J. S. Dohnanyi, *J. Geophys. Res.* **74**, 736 (1969). Although this may not be the appropriate exponent to best represent circumstellar material, we have employed it for illustrative purposes.
13. The spectroscopically determined rotation velocity cited in (*1*) can be interpreted as the star's equatorial velocity, if we can make the logical assumption that the spin axis is perpendicular to the plane of the disk. The spin angular momentum then follows when the mass, mass distribution, and radius for a typical A5V star are used.
14. V. S. Safronov, *Symposium on the Origin of the Solar System* (CNRS, Nice, 1972).
15. I. Iben, Jr., "Stellar ages," *Proc. IAU Colloq. 17* (Paris-Meudon Observatory, 1973), chapter 11.
16. The Poynting-Robertson effect describes the loss of angular momentum of an orbiting particle to a star's radiation field. The particle slowly spirals inward to the star on a time scale determined by the size, density, and distance of the particle from the star and by the luminosity of the star. See, for example, K. R. Lang, *Astrophysical Formulae* (Springer-Verlag, New York, 1980).
17. This interpretation has been proposed by D. A. Harper, R. F. Lowenstein, and J. A. Davidson [*Astrophys. J.* **285**, 808 (1984)] as an alternative to the millimeter-size particles proposed by the IRAS investigator team; see (*2*).
18. We thank R. I. Thompson for helpful discussion and F. Vilas for her contributions to the design of the Arizona cornonagraph. We also thank C. C. Avis of the Image Processing Laboratory, Jet Propulsion Laboratory, and J. W. Fountain of the Lunar and Planetary Laboratory, University of Arizona, for their assistance with some of the image processing.

4 October 1984; accepted 23 October 1984

A Circumstellar Disk Around β Pictoris

BRADFORD A. SMITH and RICHARD J. TERRILE

Science **226** (4681), 1421-1424.
DOI: 10.1126/science.226.4681.1421